



Nanocarbon and medicine: polymer/carbon nanotube composites for medical devices

Anna Prioriello^{1,2} · Laura Fazi^{2,3}  · Pietro Morales² · Leonardo Duranti³ · Davide Della Morte^{2,4} · Francesca Pacifici⁴ · Manfredi Tesauro^{2,4} · Michelina Soccio^{5,6,7} · Nadia Lotti^{5,6,8} · Laura Capozzoli⁹ · Giovanni Romanelli^{1,2} · Luca Tortora¹⁰ · Silvia Licocchia^{2,3}

Received: 1 February 2024 / Accepted: 5 July 2024 / Published online: 25 October 2024
© The Author(s) 2024

Abstract

In view of wide-ranging application to the biomedical field, this work investigates the mechanical and electrical properties of a composite made of Single Wall Carbon Nanotubes (SWCNT) bundles self-grafted onto a poly-dimethyl-siloxane (PDMS) elastomer, particularly Sylgard 184, that has well assessed biocompatible properties and is commonly used in prosthetics. Due to the potential risks associated with the use of carbon nanostructures in implanted devices, we also assess the viability of cells directly grown on such composite substrates. Furthermore, as the stability of conductive, stretchable devices made of such composite is also crucial to their use in the medical field, we investigate, by different experimental techniques, the grafting of SWCNT bundles deep into PDMS films. Our findings prove that penetration of SWCNT bundles into the polymer bulk depends on heating time and carbon nanotubes can be seen beyond 150 μm from the surface. This is confirmed by direct electron microscopy observation of large bundles as deep as about 20 μm . The composites exhibit reliable mechanical and electrical responses that are more suitable to large and repeated deformation of the polymer with respect to thermoplastic based composites, suggesting a wide potential for their application to stretchable biomedical devices. Aiming at the proposed application of artificial bladders, a bladder prototype made of poly-dimethyl siloxane endowed with a printed SWCNT-based strain sensor was developed.

Keywords Carbon nanotubes · Polymer composites · Self-assembly · Stretchable sensors · Stretchable conductors · Artificial bladder

✉ Laura Fazi
laura.fazi@uniroma2.it

¹ Department of Physics, University of Rome Tor Vergata, Rome 00133, Italy

² NAST Centre, University of Rome Tor Vergata, Rome 00133, Italy

³ Department of Chemical Science and Technologies, University of Rome Tor Vergata, Rome 00133, Italy

⁴ Department of Systems Medicine, University of Rome Tor Vergata, Rome 00133, Italy

⁵ Department of Civil, Chemical, Environmental and Materials Engineering, University of Bologna, Via Terracini 28, Bologna 40131, Italy

⁶ Interdepartmental Center for Industrial Research on Advanced Applications in Mechanical Engineering and Materials Technology, CIRI-MAM, Viale del Risorgimento 2, Bologna 40136, Italy

⁷ Interdepartmental Center for Industrial Research on Buildings and Construction CIRI-EC, Via del Lazzaretto 15/5, Bologna 40131, Italy

⁸ Interdepartmental Center for Industrial Agro-Food Research, CIRI-AGRO, Via Quinto Bucci 336, Cesena 47521, Italy

⁹ Istituto di Chimica Dei Composti OrganoMetallici (ICCOM), Consiglio Nazionale Delle Ricerche (CNR), Via Madonna Del Piano 10, Sesto Fiorentino, Firenze 50019, Italy

¹⁰ Department of Science, Roma Tre University, Via della Vasca Navale 84, Rome 00146, Italy

1 Introduction

The surging interest in stretchable conductive composite materials, adaptable to a wide spectrum of applications, has fostered the need for investigation into scalable fabrication techniques and specifically tuned geometric structures [1–3]. The combination of carbon nanotubes' conductivity and robustness with the viscoelastic properties of polymer films, particularly their stretchability, has given rise to a promising category of composite materials [4–17]. These composites, particularly those obtained by self-grafting of SWCNT on polymeric films, hold the potential of a cost-effective, conductive, elastic, mouldable, and patternable solution.

However, aiming at safe and reliable medical devices, the selection of polymers tailored to specific application (which could be more or less elastic/plastic, harder or softer, more or less conductive etc.) implies targeted studies of the penetration depth and rooting of the carbon nanotubes (CNT) intricate bundles self-grafted on the polymer film and intertwined with its macromolecular chains. Although several classical molecular dynamics simulation studies supplied very valuable information on the interactions at the level of single polymer chain with short sections of single nanotubes [18–20], the practical and exceedingly complex problem of the interaction of nanotube large and heterogeneous bundles with a bath of polymer chains remains computationally unattainable, and so far, it can only be tackled experimentally.

Recent advancement in the field of composite materials have been focused on the development of stretchable and flexible materials equipped with custom electrical properties [21, 22]. The electrical conductivity of these materials is directly influenced by the conductive component concentration, which can be tailored to make it more or less responsive to strain, to fabricate strain sensors with varying sensitivities [23]. Several established techniques are commonly employed for the analysis of these composites, such as Scanning Electron Microscopy (SEM) and Confocal Raman Spectroscopy, used for localized surface analyses and for bulk compositional investigation respectively. Moreover, the electro-mechanical characterization of the composite is necessary to tune the properties of the fabricated composite on the specific application.

In our prior research, we introduced a novel composite material comprising SWCNT self-grafted and embedded in poly-ethylene films [24, 25]. This unique combination harnessed the thermoplastic properties of the polymer while leveraging the conductive and elastic attributes of CNT bundles. Such properties were used to realize arrays of sub-millimetre conductive tracks on poly-ethylene films. These tracks could be stretched, shaped, and even implanted onto the brain cortex of laboratory rats, allowing for successful

and consistent probe of their electro-corticogram signals over the course of several months [25].

Extension of self-grafting of carbon nanotubes to thermosetting elastomers was also recently investigated in our group [26] to broaden the application area of such composites. This composite material could be built onto specific locations of artificial, fully biocompatible polymeric prostheses, to allow continuous monitoring of their state via measurement of extension, based on electrical resistance variation or, possibly, of electrical conductivity of the fluids therein exploiting the built-in composite as electrodes of high specific surface. Artificial bladder models are a first step toward the development of organs that need electrical signal transduction.

These achievements mark significant progress in the development of composite materials that bridge the areas of flexibility, electrical conduction, and biocompatibility. The potential application of such materials range from advanced medical devices to novel sensor technologies. As research in this field continues to advance, we can anticipate even more exciting breakthroughs that will shape the future of flexible and tuneable materials.

2 Materials and methods

2.1 Sylgard 184 PDMS film preparation

SYLGARD 184 silicone elastomer films were obtained by mixing base and curing agent (purchased by Sigma-Aldrich) in a ratio of 10 parts base to 1 part curing agent, by weight. After gentle mixing with a glass rod, the pressure was reduced to 5 mbar and kept for 30 min to ensure the degassing of the mixture. Afterwards, the silicone elastomer mixing was dropped on laboratory weighing boats in the minimum amount to ensure the complete covering of the surface and placed in an oven at 70 °C for 4 h (or at 100 °C for 2 h) to allow the film curing.

Through the procedure described, colorless and fully transparent films were obtained, their thickness ranging from 100 to 700 µm.

2.2 Composites preparation

In general, composite achievement by self-grafting is obtained by drop-casting a SWCNT suspension on the polymer substrate. The suspension was obtained by mixing 10 mg of SWCNT in a 10 mL water: ethanol 70:30% v/v mother solution containing 0.1 mg of surfactant, linear alkylbenzene sulphonate (LAS); this was then sonicated by a 4-hour treatment with an ultrasonic probe disintegrator (Fisher scientific Sonic Dismembrator) to obtain a more

uniform dispersion of the nanotube bundles. The obtained suspension was kept into a bath sonicator and further diluted in a 1:1 ratio in ethanol to obtain the usable suspension.

Composite specimen tracks of rectangular shape, of suitable dimension (20–30 mm long, 2–5 mm wide and 0,3–0,7 mm thick), have been prepared via the following procedure: the Sylgard film substrate was very slightly (< 1%) stretched on the round wall of a bulk aluminium cylinder and fixed by adhesive tape at its ends. A polymeric mask was also stretched over the Sylgard on the drum, so that the mask was forced to perfectly adhere to the polymeric substrate. Along the axis of the drum an electrical heater was inserted to allow for adjustment of the Sylgard film temperature. A Chromel-Alumel 0.5 mm diameter, stainless steel armoured thermocouple was inserted in a 0.6 mm diameter bore just below the drum wall surface to control and measure the temperature at which deposition was made and the subsequent heating below the melting point of the Sylgard substrate. While the temperature was kept between 80 °C and 90 °C by a Eurotherm mod. Zx controller, the nanotubes suspension was manually cast through the syringe needle in between the edges of the mask. At this temperature the solvent evaporates quickly leaving a brown/black and homogeneous deposit on the Sylgard surface. The temperature was then raised to 160 °C, well below the 200 °C threshold of loss of the mechanical properties of the elastomer [27] and maintained for a few minutes; the drum was then cooled to room temperature and the CNT track was manually brushed to remove non-adhering flakes.

When the CNT layer appeared uniformly black and flat, the mask was carefully removed from the drum and the tracks were analysed. The described deposition technique is simpler and more economic than other methods experimented to have a uniform CNT coating for large areas [28].

2.3 Electron microscopy characterization

SEM micrographs were obtained by a Tescan GAIA (3rd Series) electron microscope. Secondary electron images were collected in high-vacuum condition and with beam energy of 2 kV selecting the best trade-off in terms of electron penetration and image spatial resolution. To properly investigate the interface between SWCNTs and the polymers, sections of the composite films were analysed. Clean sections were obtained by soaking the silicone specimens in liquid nitrogen and fracturing them at the desired position with the aid of a sharp lancet.

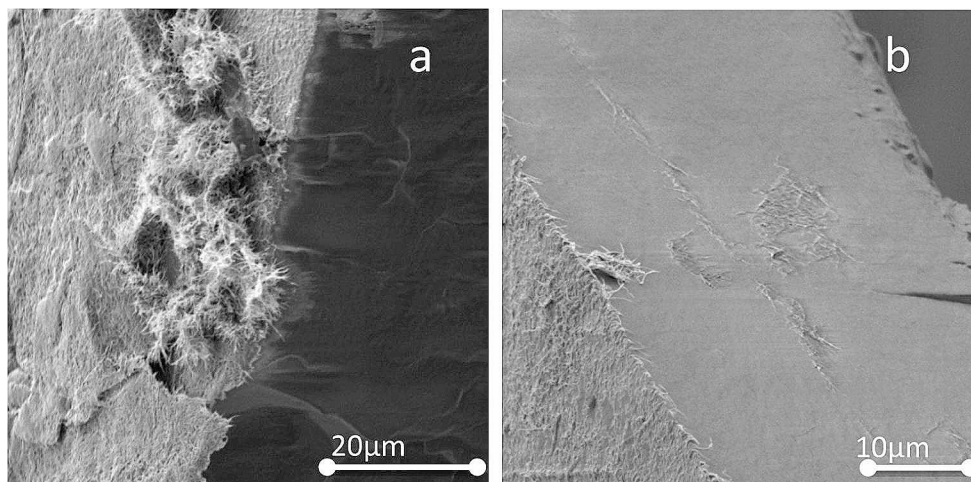
The samples were observed by tilting the SEM stage up to 70° aiming at the best orientation compromise to observe both the surface with its edge and the section showing the interface layer between the CNT and the polymers, obtaining the micrographs reported in Fig. 1.

2.4 MicroRaman composition mapping

To investigate the different CNT penetration depths, specimens were analysed by Confocal Raman Spectroscopy using a Horiba Xplora Plus instrument. Measurements used a 50X objective, laser wavelength 638 nm, grating 1200 gr/mm and were extended in the spectral range from 60 cm^{-1} to 3200 cm^{-1} . In particular, the inelastic Raman scattering signal was recorded while scanning the laser focal region along the z axis perpendicular to the sample surface: the decrease of the SWCNT Raman G band (1580–1600 cm^{-1}) intensity allows to evaluate their penetration depth. This is possible due to the high transparency of the polymer and to a careful choice of the region to be investigated, which must have a fairly low density of carbon nanotube bundles in order to cause negligible absorption of the laser beam.

We have not considered the D/G band ratio due to the unknown amount of graphite, amorphous carbon and defective nanotubes in our as grown CNT bundles.

Fig. 1 SEM investigation of SWCNT penetration in the PDMS film by observation of the specimens' section obtained by film fracture at 77 K



2.5 Electro-mechanical characterization

The electro-mechanical properties of the composite material were investigated through stress-strain, resistance-strain, and current-applied voltage cycles measurements carried out by an Elis Z20 Tensile Machine equipped with a high voltage power supply (Bertan 205 A-05R) and a digital multimeter (KDM-360CTF).

2.6 Demonstration prototype

The artificial bladder prototype was fabricated using a two-component PDMS Silicone RPRO Tech33 (purchased by Reschimica, Firenze) that has physical-chemical and mechanical properties very similar to the Sylgard-PDMS analyzed previously, even though this particular Silicone material is not yet certified for biomedical application. This choice is due to the need of obtaining easy and well assessed detachment of the model from the fabrication support. Equal volumes of base and hardener were mixed and, after 10 min of degassing, were cast on a nearly spherical inflatable support having an approximate diameter of 10 cm. After the silicone polymerization, the inflatable support was extracted from inside the silicone model and the SWCNT strain sensing conductive track was realized across a couple of copper foil electrodes sealed into the silicone model and emerging from it, following the drop casting procedure as described above.

The artificial bladder thus prepared was tested by filling and emptying it with water while recording the variable electrical resistance of a 5 mm wide, 23 mm long conductive SWCNT track.

2.7 Biocompatibility tests

2.7.1 Cell culture

The murine myoblast cell line (C2C7) was purchased from American Type Culture Collection (ATCC). Cells were cultured in high glucose Dulbecco's modified eagle's medium (DMEM) (Thermo Scientific, Waltham, MA, USA) supplemented with 20% fetal bovine serum (FBS) (Thermo Scientific, Waltham, MA, USA), 100 U/ml penicillin/streptomycin (Thermo Scientific, Waltham, MA, USA), and were maintained at 37 °C in humidified air containing 5% CO₂.

2.7.2 Cell viability assay

Cell viability was assessed by using the MTT (3-(4,5-dimethylthiazol-2-yl)-2,5-diphenyltetrazolium bromide) assay (Sigma Aldrich, Saint Louis, MO, USA), following the manufacturer's protocol [29] Briefly, 8×10^4 cells/well were

seeded into a 12 multi-well plate, containing Sylgard samples with or without nanotubes, for 24 h. Then, the medium was removed and Sylgard samples were transferred into a new 12 multi-well plate, allowing the evaluation of cell viability of those cells that adhere to the Sylgard sample and not to the plate. Subsequently, cells were incubated for 3 h at 37 °C with 5 mg/mL of MTT. After 3 h, a solution of 0.04–0.1 N HCl in isopropanol (Sigma Aldrich, Saint Louis, MO, USA) was added and the production of Formazan (a standard artificial dye used for histochemical analyses) was assessed by measuring the absorbance at 570 nm.

3 Results and discussion

3.1 Characterization of the SWCNT/PDMS composite

Safe exploiting of the electrical conduction of the SWCNT together with the mechanical properties of our elastomer in medical devices, implies a good knowledge of the self-grafted nanotubes layer morphology as well as the distribution of nanotube bundles that spontaneously “root” into the polymer surface and drift inside the polymer bulk.

3.1.1 SEM characterization

SEM characterization of the film section of the SWCNT was carried out to analyse the concentration gradient in the PDMS matrix along the direction perpendicular to the polymer film surface. Figure 1 reports details of the section at two different magnifications. The distribution of the nanotube bundles and flakes at the surface of the film is inhomogeneous since it arises from drop casting of a non-uniform suspension. Consequently, the concentration of SWCNT in the polymer bulk is also not uniform and varies from one section to another. Figure 1a shows a detail of the drop cast SWCNT layer and of the section fracture, where one can see that most of the nanotube layer is completely soaked by the polymer. Figure 1b shows a representative example of the mentioned inhomogeneity in the polymer film body: apart from a CNT flake hanging from the surface on the section (at the left), we see the section of a first flake about 7–8 μm deep in the film (i.e. to the right in the figure) followed by an approximately 50 μm long thin layer parallel to the surface and approximately 10 μm deep, and by a further thicker bundle whose section extends from 12 to 18 μm in depth and 10 μm in length. Similar uneven distributions of CNT that have diffused from the surface into the bulk can be observed in most sections. Note that CNT bundles observed in the polymer bulk look very different from the isolated flakes deposited on the surface, as the former, like

most of the surface SWCNT layer, are wet and entangled in the polymer chains that also diffuse into the bundles. Such appearance has also been observed for CNT embedded in poly-urethane [30]. Due to such uneven distribution of the CNT bundles in the polymer, SEM does not appear to be the best technique to determine an average concentration gradient. Still, the important result obtained on this specific sample section, is that even fairly large flakes can penetrate at least 18 μm in the 25 μm thick film.

3.1.2 Confocal MicroRaman characterization

Further information on the self-grafting and diffusion processes of CNT into the polymer matrix can be obtained by confocal micro Raman spectroscopy, exploiting the transparency of the Sylgard 184 film and looking at the Raman spectral fingerprints of both SWCNT and Sylgard as a function of the z coordinate (perpendicular to the film surface). This technique therefore does not need analysis of macroscopically realized sections, since z direction scans can be performed on any suitably chosen microscopic area of the specimen.

Figure 2 reports the inelastic Raman spectra of the individual components and of the composite film over the range 60–3200 wavenumbers from the laser excitation energy. Since the composite is prepared at a temperature of 160 $^{\circ}\text{C}$, the spectrum of the pure polymer film heated at such temperature is also shown.

The thermal treatment does not affect the vibrational dynamics of the polymer, as no appreciable difference is observed in the explored spectral range of pristine or heated samples.

When recorded as a function of the z coordinate, such spectral fingerprints of the materials in the composite supply

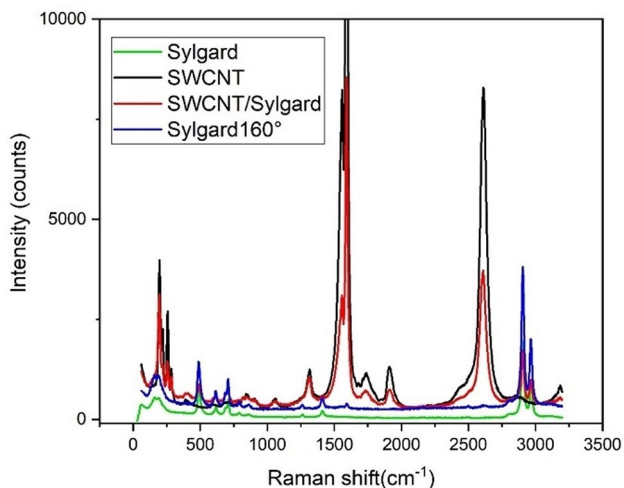


Fig. 2 Inelastic Raman spectra of the PDMS film grafted SWCNT (in red) compared to pure PDMS, heated PDMS and pure SWCNT

a direct information on the penetration depth of SWCNT that are initially drop cast on one face of the film, and drift into the polymer substrate to an extent to be determined; this extent increases, at least for thermoplastic polymers, if the film is heated close to the melting temperature for some time after the deposition of the SWCNT suspension [31].

Figure 3a shows plots of the integral of the Raman G band signal of SWCNT (full squares) in the spectral window between 1500 cm^{-1} and 1600 cm^{-1} and of the integral of the 2900 cm^{-1} Raman band signal of Sylgard (full triangles) CH_2 stretching mode, between 2800 and 3000 cm^{-1} . Measurements were performed on composite samples with thickness varying between 130 μm and 400 μm approximately. After drop casting of the SWCNT suspension, samples were heated to a maximum of 160 $^{\circ}\text{C}$ to avoid the damaging of the polymer structure, reported to occur above 200 $^{\circ}\text{C}$ [32].

The spectra show that, after cooling to room temperature, the concentration of SWCNT is maximum at the edge of the film, where they are drop cast, and decreases in the Sylgard bulk. This measurement was repeated on samples heated for different times, from 30 s to 180 min. Figure 3b shows the SWCNT signal intensity at a depth of 25 μm (where separation of the different curves of Fig. 3a is maximum) as a function of the heating time. We can see that the penetration depth can be extended by approximately 35–40% by heating for extended times.

The effect of heating time can be still observed at a depth of 100 μm and more.

It must be underlined that these data cannot be considered quantitative because of: (a) the inhomogeneous nature of the CNT bundles in the polymer; (b) the absorbance of the laser beam by such inhomogeneous distribution, which affects the Raman scattering signal. Furthermore, we have observed that the polymer substrate becomes slightly opalescent and less transparent with long heating times thus scattering part of the laser beam; this may account for the anomalous decrease of the polymer signal with prolonged heating.

Despite the described warnings, both SEM and Raman results are in agreement with previous work on other polymeric substrates [31] and describe a fully consistent picture of SWCNT self-grafting and deep penetration in the Sylgard polymer.

3.1.3 Electro-mechanical characterization

The investigation of the mechanical and electrical properties of the developed composite films is necessary in view of their use to develop elastic prosthetic devices endowed with built-in sensors and electrical connections.

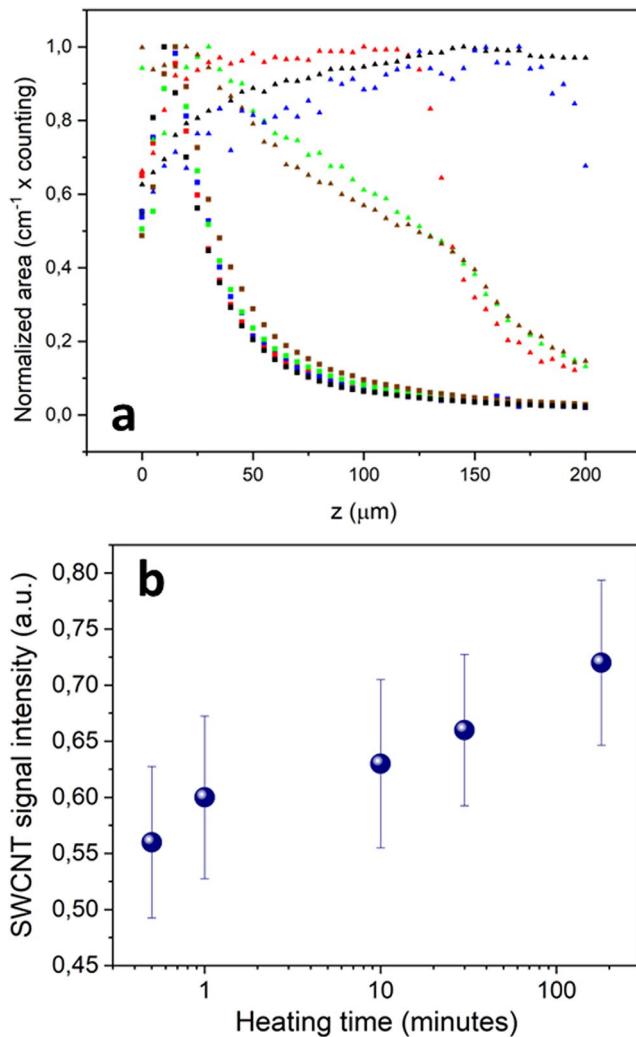


Fig. 3 (a) Concentration of carbon nanotubes and polymer molecules inside the composite film vs. distance from the deposition surface, for different heating times. Note that the thickness is not the same for all specimens and ranges from 130 to 400 μm. Symbols are as follows: triangles refer to the Sylgard substrate and squares refer to SWCNT; colours refer to different heating times: black = 30 s, red 1 min, blue 10 min, green 30 min, brown 180 min. (b) concentration of Carbon nanotubes at a depth of 25 μm vs. sample heating time

Figure 4 shows that 6 cycles of stress/strain measurements performed over a strain up to $(\Delta L)/L = 40\%$ (i.e. stretching the film to 140% of the initial length) are perfectly reproducible with only minimal hysteresis. The plot shows that there are no significant differences between the first three cycles and three subsequent cycles performed after relaxing the sample for 15 h with no strain.

It is however peculiar that the corresponding resistance/strain plot, reported in red in Fig. 5a, shows a deviation of the resistance, on releasing the strain below 30%, the final resistance remaining approximately 6% higher. The choice of plotting resistance, rather than resistivity, is due to the fact that the latter is affected by a large error due to uneven

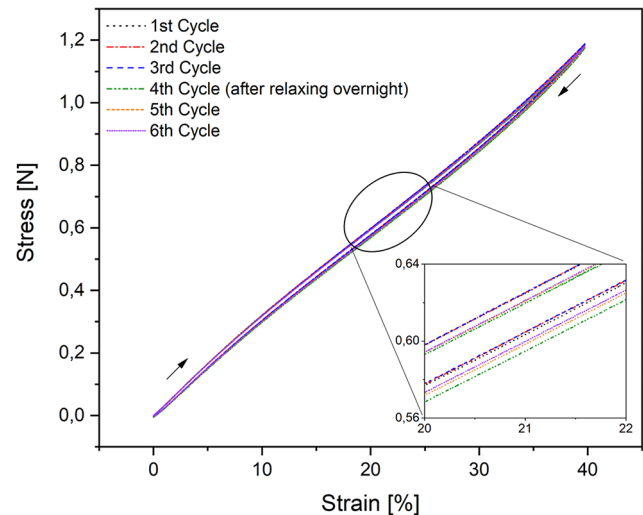


Fig. 4 Cyclic stress/strain test of a conductive track of the following dimensions: 27 mm long, 3 mm wide and 0,7 mm thick

thicknesses both of the polymer film and of the SWCNT conductive filler penetration depth. The observed behaviour might be due to the decrease of the number of conductor-to-conductor electrical contacts and/or tunnelling junctions caused by the rapid filling by the polymer of the spaces between individual conductive components created by straining the composite material.

Similar electrical conduction mechanisms have also been suggested by Lee et al. [27]. Figure 5b demonstrates that several consecutive strain/release cycles in the strain range 0–40% of the SWCNT/Sylgard PDMS composite, show a fairly repeatable behaviour, with only minor resistance variations, of about 5% at most. Once again, this behaviour is maintained after several hours of molecular relaxation in the unstrained condition. Thus, although the electrical conduction of our composite is slightly less stable compared to its stress vs. strain behaviour, it seems perfectly suitable for most application fields. The sensitivity of the linear part of the plot is about 10 kOhm/(% Strain); this was measured on a 24 mm long – 3 mm wide conductive sample. Similar results were obtained for samples of the similar sizes.

Figure 6 reports the I/V plot for different strain values measured to check the conduction behaviour of the devices at different applied voltages. The plots are basically linear, although the voltage decrease after reaching a maximum of 200 V causes a very slightly lower current to flow in the carbon nanotubes component. No qualitative deviation from a simple ohmic behaviour is however observed even on a stretched conductor.

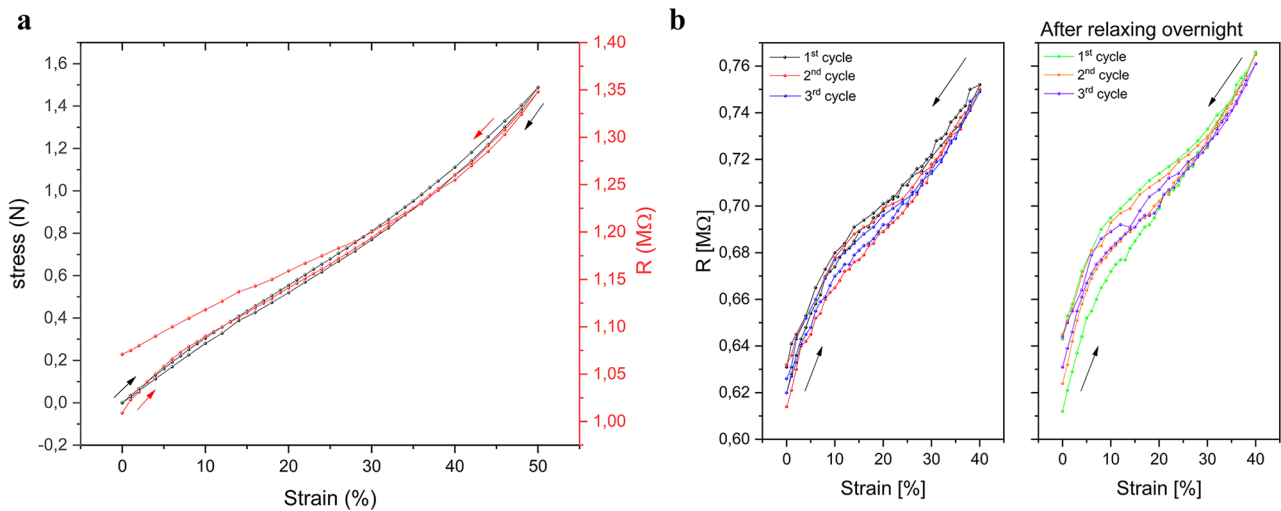


Fig. 5 (a) Resistance and stress/strain test on one cycle; (b) Resistance/strain test on three cycles, on a new specimen and on the same specimen after 15 h of relaxation at the original unstretched length

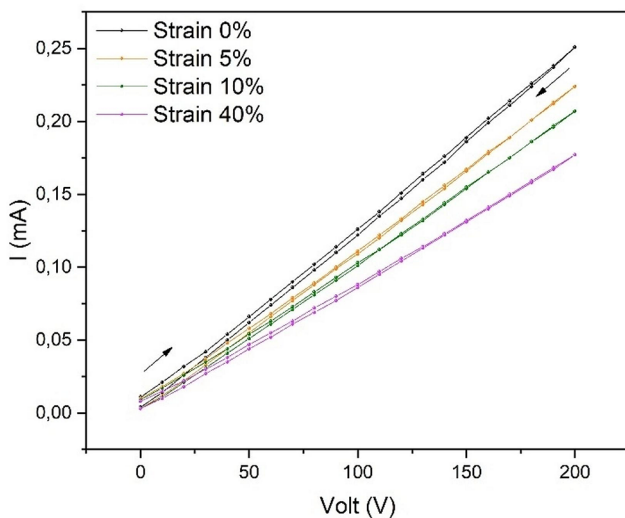


Fig. 6 I/V test of a conductive track of the following dimensions: 24 mm long, 3 mm wide and 0,4 mm thick

3.2 Biocompatibility results

The effect of nanotubes on cell viability has been the object of extensive research for many years, in particular in so far as neuronal cells are concerned [33–37]. It was found that not only CNT maintain cell viability, but it is also an excellent growth substrate, so that it is used in technological neuronal application. *In vivo*, long term experiments [31] demonstrated the viability for at least 11 weeks of a composite material based on SWCNT and poly-ethylene, whose structural properties however are different from those of the SWCNT/elastomer composite. More recent work has used successfully CNT transferred onto PDMS films as flexible implantable electrodes [38], with excellent biocompatibility

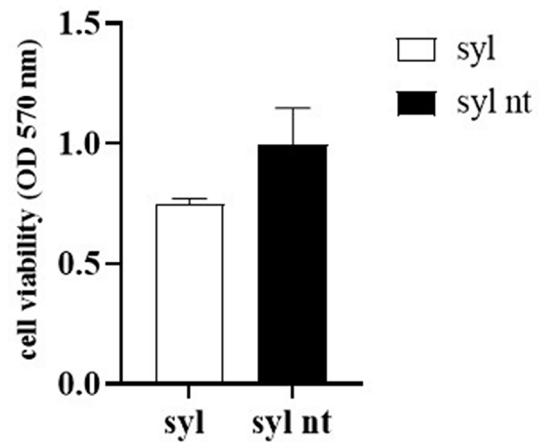


Fig. 7 Cell viability was assessed on a murine myoblast cell line, C2C7, plated on Sylgard samples with or without nanotubes. Data are reported as mean \pm Standard Error of Measurement (number of samples=3). OD: optical density

over a period of 2 weeks. As a step forward we need to understand the cell viability *in vitro* on our SWCNT/Sylgard 184 elastomer composite, where the substrate structure is different from other studies. We therefore performed an MTT assay, as detailed in the [Materials and Methods](#) section, to analyse the viability of cells grown on SWCNT self-grafted on Sylgard 184.

Figure 7 shows that there were no significant differences in cell viability between the cells plated on Sylgard and those plated on Sylgard with nanotubes, suggesting that the presence of nanotubes did not have an adverse impact on cell viability and function. To mitigate potential cell-specific effects, we also used a murine neuroblastoma cell line, N1E115, obtaining consistent results.

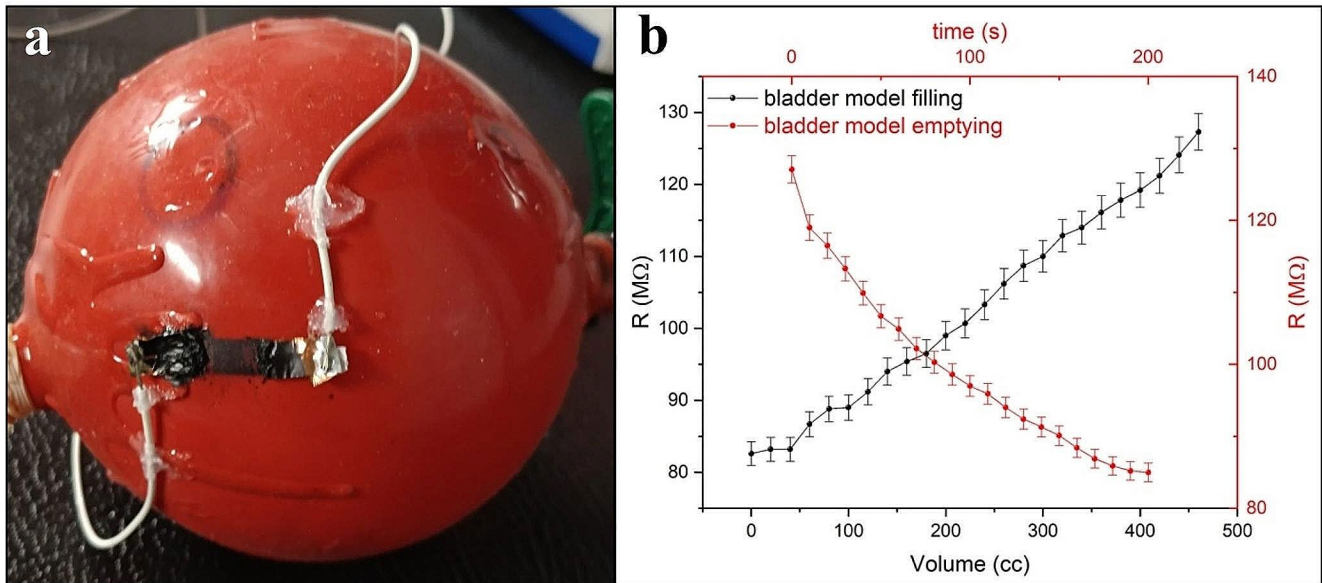


Fig. 8 (a) A PDMS bladder model endowed with a printed and self-grafted SWCNT strain, connected by the two white wires soldered to built-in copper electrodes; (b) Resistance of the strain sensor of the

PDMS model bladder, vs. filling (24 stepwise fillings, by 20 cc each, black dots), and vs. continuous emptying at a rate of 2.4 cc/s (red dots)

3.3 Application example: artificial bladder prototype development

Having assessed the stability of the composite and its promising mechanical and electrical properties, we developed a prototype model of an artificial bladder silicone based, endowed with SWCNT built-in sensors of the strain due to urine filling. Other devices, such as electrical conductivity, turbidity, and pH sensors, can be implemented using the same methodologies. The strain sensor was “printed” on the outer and lower part of the model, by the described method of drop casting through a mask, to record the complete process of filling and emptying.

Figure 8a shows a photograph of the laboratory prototype model bladder with a detail of the strain sensor electrical connection. Figure 8b shows the increasing (on water filling) and decreasing (on water emptying) resistance values. Note that each 20 cc stepwise filling was followed by a signal stabilization time of approximately 60 s, after which the resistance value remained stable and the next 20 cc amount of water was added. The resistance shows a fairly smooth increase on filling and an even smoother behaviour on emptying, offering useful data for the development of the artificial model bladder.

4 Conclusions

Self-grafting of SWCNT on polymers represents an easy way to accomplish electric sensors and electrodes with different viscoelastic properties depending on the application.

The body of results converges to indicate that stable conductive and stretchable composites can be fabricated by depositing Single Wall Carbon Nanotubes on the biocompatible, well assessed Poly-Dimethyl Siloxane (Sylgard 184) thermosetting elastomer substrate. SEM and Raman analysis indicate a deep penetration of SWCNT bundles into the polymer, leading to a safe material suitable to the fabrication of biomedical implantable devices.

The composite is stable, has repeatable and reliable properties and is fully biocompatible as the cell viability tests demonstrated. The body of previous available results confirms the present in vitro studies: in a different work we demonstrated that subdural electrodes made of SWCNT self-grafted onto poly-ethylene (another biocompatible substrate) did not have adverse effects on the health and behaviour of freely moving laboratory rats [31] for at least 11 weeks. A different investigation conducted in vivo using carbon nanotubes transferred from a lithographic substrate to PDMS films showed good biocompatibility although the experiments were only carried on for 2 weeks. Moreover, it has been reported that Mesenchymal Stem Cells adhere to the substrate for at least 7 days before inducing their differentiation into osteoclasts [39]. Also, following the differentiation, cells remains adherent to the substrate, suggesting that the composite does not interfere with long

term cellular functions and/or viability [40, 41]. We have therefore exploited such properties to fabricate a silicone-based prototype of artificial bladder endowed with built-in filling level sensors with which we have measured repeated cycles of filling and emptying. This technology turns out to be reliable and economic, and it is particularly promising for devices needing easy and inexpensive micro-patterning of the conductive path and therefore for further development of several types of artificial prostheses. Furthermore, it can be extended to a wider application field on exploiting different polymers, and in particular the more mouldable thermoplastic ones that can be adapted to specific shape (as already demonstrated in neurological application), or harder but flexible ones where electrical signals need to be transferred over movable or vibrating parts.

Several directions of this research are foreseeable: 1) extending the application range into both implantable sensors and active transduction of signals, 2) extending the range of polymeric materials suitable for both implantation and the required application, 3) understanding the interaction mechanisms between carbon nanotubes and the different polymers, and at last 4) understanding if the interaction of high specific surface CNT/polymer composites with gaseous and liquid analytes can affect their electrical conductivity.

Acknowledgements The authors gratefully acknowledge Regione Lazio POR FESR Lazio 2014-2020-PROGETTI DI GRUPPI DI RICERCA 2020 CUP: E85F21001030002; (G10795 published by BURL n. 69, 27/08/2019). The authors gratefully acknowledge the support of the ISIS@MACH ITALIA Research Infrastructure, the hub of ISIS Neutron and Muon Source (UK), [MUR official registry U. 0008642.28-05-2020 – 16th April 2020].

Funding Open access funding provided by Università degli Studi di Roma Tor Vergata within the CRUI-CARE Agreement.

Open Access This article is licensed under a Creative Commons Attribution 4.0 International License, which permits use, sharing, adaptation, distribution and reproduction in any medium or format, as long as you give appropriate credit to the original author(s) and the source, provide a link to the Creative Commons licence, and indicate if changes were made. The images or other third party material in this article are included in the article's Creative Commons licence, unless indicated otherwise in a credit line to the material. If material is not included in the article's Creative Commons licence and your intended use is not permitted by statutory regulation or exceeds the permitted use, you will need to obtain permission directly from the copyright holder. To view a copy of this licence, visit <http://creativecommons.org/licenses/by/4.0/>.

References

1. M. Rossi, M. Meo, On the estimation of mechanical properties of single-walled carbon nanotubes by using a molecular-mechanics based FE approach, *Spec. Issue 12th Eur. Conf. Compos. Mater. ECCM 2006*, vol. 69, no. 9, pp. 1394–1398, 2009, <https://doi.org/10.1016/j.compscitech.2008.09.010>
2. B.C.K. Tee, J. Ouyang, Soft electronically functional polymeric composite materials for a flexible and Stretchable Digital Future. *Adv. Mater.* **30**(47), 1–14 (2018). <https://doi.org/10.1002/adma.201802560>
3. M. Abbas, M.N. Ahmad, T. Hussain, A. Mujahid, Materials for wearable sensors. *Mater. Innov.* **2**(7) (2022). <https://doi.org/10.54738/mi.2022.2702>
4. Y. Xiao, Z. Li, C. Hu, L. Yang, D. Zhang, A stretchable flexible strain sensor with high sensitivity and fast response fabricated by embedded 3D printing of the hybrid polydimethylsiloxane/conductive carbon paste composites. *J. Appl. Polym. Sci.* (2024). <https://doi.org/10.1002/app.55558>
5. Z. Qiao, A. Wei, K. Wang, N. Luo, Z. Liu, Study of flexible piezoresistive sensors based on the hierarchical porous structure CNT/PDMS composite materials. *J. Alloys Compd.* **917** (Oct. 2022). <https://doi.org/10.1016/j.jallcom.2022.165503>
6. Y. Zhao et al., Dec., Advancing the pressure sensing performance of conductive CNT/PDMS composite film by constructing a hierarchical-structured surface, *Nano Mater. Sci.*, vol. 5, no. 4, pp. 343–350, 2023, <https://doi.org/10.1016/j.nanoms.2021.10.002>
7. P. Ananthasubramanian, R. Sahay, N. Raghavan, Investigation of the surface mechanical properties of functionalized single-walled carbon nanotube (SWCNT) reinforced PDMS nanocomposites using nanoindentation analysis. *RSC Adv.* **14**(22), 15249–15260 (2024). <https://doi.org/10.1039/D4RA02717E>
8. Z. Zhang et al., A pressure and temperature dual-parameter Sensor based on a Composite Material for Electronic Wearable devices. *Micromachines.* **14**(3) (Mar. 2023). <https://doi.org/10.3390/mi14030690>
9. J. Sanguantrakul, A. Hemakom, P. Israsena, The Development of Low-Cost Dry Electrode using PDMS/CNT Composite, in *2023 3rd International Symposium on Instrumentation, Control, Artificial Intelligence, and Robotics, ICA-SYMP 2023*, 2023, pp. 37–40, <https://doi.org/10.1109/ICA-SYMP56348.2023.10044944>
10. G. Matzeu, A. Pucci, S. Savi, M. Romanelli, F. Di Francesco, A temperature sensor based on a MWCNT/SEBS nanocomposite. *Sens. Actuators Phys.* **178**, 94–99 (2012). <https://doi.org/10.1016/j.sna.2012.02.043>
11. A. Giuliani, M. Placidi, F. Di Francesco, A. Pucci, A new polystyrene-based ionomer/MWCNT nanocomposite for wearable skin temperature sensors. *React. Funct. Polym.* **76**(1), 57–62 (2014). <https://doi.org/10.1016/j.reactfunctpolym.2014.01.008>
12. Z.F. Liu et al., Hierarchically buckled sheath-core fibers for superelastic electronics, sensors, and muscles, *Science (80-)*, vol. 349, no. 6246, pp. 400–404, 2015, <https://doi.org/10.1126/science.aaa7952>
13. B. Pradhan, R.R. Kohlmeyer, K. Setyowati, H.A. Owen, J. Chen, Advanced carbon nanotube/polymer composite infrared sensors. *Carbon N Y.* **47**(7), 1686–1692 (2009). <https://doi.org/10.1016/j.carbon.2009.02.021>
14. H. Stoyanov, M. Kollosche, S. Risse, R. Waché, G. Kofod, Soft conductive elastomer materials for stretchable electronics and voltage controlled artificial muscles. *Adv. Mater.* **25**(4), 578–583 (2013). <https://doi.org/10.1002/adma.201202728>
15. A. Shoval, C. Adams, M. David-Pur, M. Shein, Y. Hanein, E. Sernagor, Carbon nanotube electrodes for effective interfacing with retinal tissue, *Front. Neuroeng.*, vol. 2, no. APR, pp. 1–8, 2009, <https://doi.org/10.3389/neuro.16.004.2009>
16. N.K. Chang, C.C. Su, S.H. Chang, Fabrication of single-walled carbon nanotube flexible strain sensors with high sensitivity. *Appl. Phys. Lett.* **92**(6) (2008). <https://doi.org/10.1063/1.2841669>
17. J. Li et al., Flexible strain sensors with high sensitivity and large monitoring range prepared by biaxially stretching conductive

- polymer composites with a bilayer structure, *J. Appl. Polym. Sci.*, no. September, pp. 1–11, 2023, <https://doi.org/10.1002/app.54718>
18. S.S. Tallury, M.A. Pasquinelli, Molecular dynamics simulations of flexible polymer chains wrapping single-walled carbon nanotubes. *J. Phys. Chem. B* **114**(12), 4122–4129 (2010). <https://doi.org/10.1021/jp908001d>
 19. L. Guo et al., Molecular dynamics simulation of the effect of the thermal and mechanical properties of addition liquid silicone rubber modified by carbon nanotubes with different radii, *E-Polymers*, vol. 23, no. 1, 2023, <https://doi.org/10.1515/epoly-2022-8105>
 20. X. Shi, X. He, X. Liu, Role of the Carbon Nanotube Junction in the mechanical performance of Carbon Nanotube/Polyethylene nanocomposites: a Molecular Dynamics Study. *Nanomaterials*. **14**(6) (2024). <https://doi.org/10.3390/nano14060520>
 21. L. Hu, B.J. Kim, S. Ji, J. Hong, A.K. Katiyar, J.H. Ahn, Smart electronics based on 2D materials for wireless healthcare monitoring. *Appl. Phys. Rev.* **9**(4) (2022). <https://doi.org/10.1063/5.0104873>
 22. A. Alrai, E. Beyhan, A. Asadi, E. Ozden-Yenigun, H. Cebeci, Tailoring piezoresistive response of carbon nanotubes sensors by hybridization of cellulose nanocrystals for composite structures, *Sensors Actuators A Phys*, vol. 362, no. October 2022, p. 114633, 2023, <https://doi.org/10.1016/j.sna.2023.114633>
 23. N. Hu et al., Investigation on sensitivity of a polymer/carbon nanotube composite strain sensor. *Carbon N Y*. **48**(3), 680–687 (2010). <https://doi.org/10.1016/j.carbon.2009.10.012>
 24. P. Morales et al., Self-grafting carbon nanotubes on polymers for stretchable electronics. *Eur. Phys. J. Plus*. **133**(6) (2018). <https://doi.org/10.1140/epjp/i2018-12040-0>
 25. L. Fazi et al., Carbon Nanotube-based Stretchable Hybrid Material Film for Electronic Devices and Applications. *J. Nanosci. Nanotechnol.* **20**, 4549–4556 (2020). <https://doi.org/10.1166/jnn.2020.17874>
 26. L. Fazi et al., Characterization of Conductive Carbon Nanotubes/Polymer composites for Stretchable sensors and transducers. *Molecules*. **28**(4), 1–13 (2023). <https://doi.org/10.3390/molecules28041764>
 27. D.K. Lee, J. Yoo, H. Kim, B.H. Kang, S.H. Park, Electrical and Thermal properties of Carbon Nanotube Polymer composites with various aspect ratios. *Mater. (Basel)*. **15**(4) (2022). <https://doi.org/10.3390/ma15041356>
 28. R. Tenent et al., May., Ultrasoft, Large-Area, High-Uniformity, Conductive Transparent Single-Walled-Carbon-Nanotube Films for Photovoltaics Produced by Ultrasonic Spraying, *Adv. Mater.*, vol. 21, pp. 3210–3216, 2009, <https://doi.org/10.1002/adma.200803551>
 29. F. Pacifici et al., The Protective Effect of a Unique Mix of polyphenols and micronutrients against Neurodegeneration Induced by an in vitro model of Parkinson's Disease. *Int. J. Mol. Sci.* **23**(6), 1–14 (2022). <https://doi.org/10.3390/ijms23063110>
 30. M.H. Jomaa et al., Investigation of elastic, electrical and electro-mechanical properties of polyurethane/grafted carbon nanotubes nanocomposites. *Compos. Sci. Technol.* **121**, 1–8 (2015). <https://doi.org/10.1016/j.compscitech.2015.10.019>
 31. L. Pavone et al., Chronic neural interfacing with cerebral cortex using single-walled carbon nanotube-polymer grids. *J. Neural Eng.* **17**(3) (2020). <https://doi.org/10.1088/1741-2552/ab98db>
 32. I.D. Johnston, D.K. McCluskey, C.K.L. Tan, M.C. Tracey, Mechanical characterization of bulk Sylgard 184 for microfluidics and microengineering. *J. Micromechanics Microengineering*. **24**(3) (2014). <https://doi.org/10.1088/0960-1317/24/3/035017>
 33. T. Gabay et al., Electro-chemical and biological properties of carbon nanotube based multi-electrode arrays. *Nanotechnology*. **18**(3) (2007). <https://doi.org/10.1088/0957-4484/18/3/035201>
 34. B. Levit, P.F. Funk, Y. Hanein, Soft electrodes for simultaneous bio-potential and bio-impedance study of the face. *Biomed. Phys. Eng. Express*. **10**(2) (2024). <https://doi.org/10.1088/2057-1976/ad28cb>
 35. I. Vèbraitè, C. Bar-Haim, M. David-Pur, Y. Hanein, Bi-directional electrical recording and stimulation of the intact retina with a screen-printed soft probe: a feasibility study. *Front. Neurosci.* **17** (2023). <https://doi.org/10.3389/fnins.2023.1288069>
 36. I. Vèbraitè, Y. Hanein, Soft Devices for High-Resolution Neuro-Stimulation: The Interplay Between Low-Rigidity and Resolution, *Front. Med. Technol.*, vol. 3, no. June, pp. 1–23, 2021, <https://doi.org/10.3389/fmedt.2021.675744>
 37. I. Vèbraitè, M. David-Pur, D. Rand, E.D. Glowacki, Y. Hanein, Electrophysiological investigation of intact retina with soft printed organic neural interface. *J. Neural Eng.* **18**(6) (2021). <https://doi.org/10.1088/1741-2552/ac36ab>
 38. H. Yang et al., Carbon Nanotube array-based flexible multifunctional electrodes to record Electrophysiology and ions on the cerebral cortex in Real Time. *Adv. Funct. Mater.* **32**(38), 1–10 (2022). <https://doi.org/10.1002/adfm.202204794>
 39. D. Jamal, R. C. De Guzman, silicone substrate with collagen and carbon nanotubes exposed to pulsed current for MSC osteo-differentiation. *Int. J. Biomater.* 3684812 (2017). <https://doi.org/10.1155/2017/3684812>
 40. A. Markov et al., Dec., Biocompatible swcnt conductive composites for biomedical applications, *Nanomaterials*, vol. 10, no. 12, pp. 1–16, 2020, <https://doi.org/10.3390/nano10122492>
 41. J.S. Yan et al., Mar., Biocompatibility studies of macroscopic fibers made from carbon nanotubes: Implications for carbon nanotube macrostructures in biomedical applications, *Carbon N. Y.*, vol. 173, pp. 462–476, 2021, <https://doi.org/10.1016/j.carbon.2020.10.077>

Publisher's Note Springer Nature remains neutral with regard to jurisdictional claims in published maps and institutional affiliations.